Proceedings of AVEC '06
The 8th International Symposium on Advanced Vehicle Control, August 20-24, 2006, Taipei, Taiwan
AVEC060091

Optimal Design of a Hybrid Solar Vehicle

I.Arsie, G.Rizzo, M.Sorrentino
Department of Mechanical Engineering, University of Salerno, 84084 Fisciano (SA), Italy

Keywords: Hybrid Vehicle, Solar Energy

I. INTRODUCTION

In the last years, increasing attention has been spent towards the applications of solar energy to cars. Various solar car prototypes have been built and tested, mainly for racing and demonstrative purposes [1] [2].
Despite of significant technological efforts and some spectacular outcomes, several limitations, such as low power density, unpredictable availability of solar source and energetic drawbacks (i.e. increase in weight and friction and aerodynamic losses due to additional components), cause pure solar cars to be still far from practical feasibility. On the other hand, the concept of a hybrid electric car assisted by solar panels appears more realistic [3][4][5][6][7]. In fact, due to relevant research efforts [8], in the last decades Hybrid Electric Vehicles (HEV) have evolved to industrial maturity. These vehicles now represent a realistic solution to important issues, such as the reduction of gaseous pollution in urban drive as well as the energy saving requirements. Moreover, there is a large number of drivers utilizing daily their car for short trips with limited power. Some recent studies, conducted by the UK government, report that about 71% of UK users reach their office by car, and 46% of them have trips shorter than 20 min, mostly with only one person on board [9]. The above considerations open promising perspectives with regard to the integration of solar panels with "pure"-electric hybrid vehicles (i.e. "tri-hybrid" cars), with particular interest in the opportunity of storing energy even during parking phases.
In spite of their potential interest, solar hybrid cars have received relatively little attention in literature [7]. An innovative prototype has been developed at Western Washington University [5][6] in the 90s, adopting advanced solutions for materials, aerodynamic drag reduction and PV power maximization with peak power tracking. Other studies and prototypes on solar hybrid vehicles have been presented by Japanese researchers [3][4] and at the Queensland University [10].
Although these works demonstrate the general feasibility of such an idea, detailed presentation of results and performance, along with a systematic approach to solar hybrid vehicle design, seem still missing in literature. Therefore, suited methodologies are required to address both the rapid changes in the technological scenario and the increasing availability of innovative, more efficient components and solutions. A specific difficulty in developing an HSV model relates to the many mutual interactions between energy flows, power-train balance of plant and sizing, vehicle dimension, performance, weight and costs, whose connections are much more critical than in either conventional or hybrid electric vehicles. Preliminary studies on energy flows in an HSV has been recently developed by the authors [11][12]. The current paper presents a more detailed study on the optimal sizing of a solar hybrid car. The optimization analyses are based on a longitudinal vehicle dynamics model, developed to account for, besides the impact of weight and costs, also the influence of energy flows and adopted control strategies.

II. STRUCTURE OF THE SOLAR HYBRID VEHICLE

Different architectures can be applied to HEVs: series, parallel, and parallel-series. These two latter structures have been utilized for two of the most diffused hybrid cars in the market: Toyota Prius (parallel-series) and Honda Civic (parallel). Instead, for solar hybrid vehicles the series structure seems preferable [7], due to its simplicity, as in some recent prototypes of HSV [10]. With this approach, the Photovoltaic Panels (PV) concur with the Electric Generator EG, powered by the ICE, to recharge the battery pack B in both parking mode and driving conditions, through the electric node EN. The electric motor EM can either provide the mechanical power for the propulsion or restore part of the braking power during regenerative braking (FIG. 1). In this structure, the thermal engine can work mostly at constant power (P_{AV}), corresponding to its optimal efficiency, while the electric motor EM can reach a peak power P_{max}:

$$P_{\max} = \theta P_{av} \tag{1}$$

FIG. 1 - SCHEME OF THE SERIES HYBRID SOLAR VEHICLE

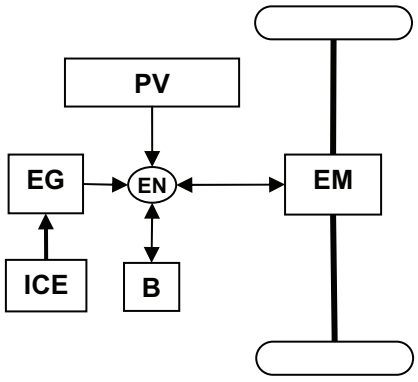

In order to estimate the net solar energy captured by PV panels in real conditions (i.e. considering clouds, rain etc.) and available for propulsion, a solar calculator developed at the US National Renewable Energy Lab has been used [13], considering four different US

locations, ranging from 21° to 61° of latitude, based on 1961-1990 time series. The calculator provides the net solar energy for different panel positions: with 1 or 2 axis tracking mechanism or for fixed panels, at various tilt and azimuth angles.

The most obvious solution for solar cars is the location of panels on roof and bonnet, at almost horizontal position. Nevertheless, two additional options have been considered: (i) horizontal panels (on roof and bonnet) with one tracking axis, in order to maximize the energy captured during parking mode; (ii) panels located also on car sides and rear at almost vertical positions. The maximum panel area can be estimated as function of car dimensions and shape, with a simple geometrical model [12].

The energy from PV panels can be obtained summing up the contribution from parking (p) and driving (d) periods. While in the former case it is reasonable to assume that the PV array has an unobstructed view of the sky, this hypothesis could fail in most driving conditions. Therefore, the energy captured during driving can be reduced by a factor $\beta<1$. In order to estimate the fraction of daily solar energy captured during driving hours (h_d), it is assumed that the daily solar energy is distributed over h_{sun} hours. A factor $\alpha<1$ is then introduced to account for further degradation due to charge and discharge processes in the battery for energy taken during parking. The net solar energy available for propulsion, stored during both parking and driving modes, can therefore be expressed as:

$$E_{s,p} = \eta_p A_{PV} e_{sun} \frac{h_{sun} - h_d}{h_{sun}} \alpha \tag{2}$$

$$E_{s,d} = \eta_p A_{PV} e_{sun} \frac{h_d}{h_{sun}} \beta \tag{3}$$

Where e_{sun} is the average daily energy captured by solar panels in horizontal position. Hereinafter, e_{sun} is assumed equal to 4.3 kWh/day, which corresponds roughly to a latitude of 30° in June month. The energy required to drive the vehicle during the day can be expressed as function of the average positive power P_{av} and the driving hours h_d:

$$E_d = \int_{h_d} P(t) \cdot dt = h_d P_{av} \tag{4}$$

The instantaneous power can be computed starting from a given driving cycle, for assigned vehicle data, integrating a vehicle longitudinal dynamic model. Required driving energy E_d depends therefore on vehicle weight and vehicle cross section, which in turn depend on the sizing of the propulsion system components and on vehicle dimensions, related to solar panel area. The contribution of solar energy to the propulsion can be therefore determined as:

$$\lambda = \frac{E_{sun}}{E_d} = \frac{E_{s,p} + E_{s,d}}{E_d} \tag{5}$$

The fuel consumption for both conventional vehicle (ICE) and HSV can be then computed and compared. Of course, in parallel with fuel saving, corresponding reduction in pollutants and CO_2 emissions with respect to the conventional vehicle is also achieved.

III. WEIGHT MODEL

A parametric model for the weight of an HSV can be obtained adding the weight of the specific components (PV panels, battery pack, ICE, Generator, Electric Motor, Inverter) to the weight of the HSV body. This latter has been obtained starting from a statistical analysis of small commercial cars (CC). A linear regression analysis has been performed, considering weight W ($W_{body,CC}$), power P and vehicle dimensions (length l, width w, height h and their product $V=lwh$) for 15 commercial cars, with power ranging from 9.5 kW to 66 kW [12]. In order to use these data to estimate the base weight of the HSV ($W_{body,HSV}$), the contribution of the components not present in the series hybrid vehicle (i.e. gearbox, clutch) has been subtracted. The CC car body also includes other components (thermal engine, electric generator, battery) that will be considered separately for the hybrid car model; the weight of ICE is estimated as function of peak power, whereas the influence of electric generator and battery has been neglected (their weights are of course much lower than the corresponding components needed on the hybrid car).

TAB. I – REGRESSION ANALYSIS FOR COMMERCIAL CAR BODY MASS.

#	Variables	R^2
1	$W=k_1+k_2P$	0.894
2	$W= k_1+k_2P+k_3l+k_4w+k_5h$	0.973
3	$W= k_1+k_2P+k_3V$	0.946

A subtractive term (ΔW) has been introduced to include weight savings achievable through the use of aluminum instead of steel for chassis: in this case, additional costs have been considered in the cost model [13]. Thus, the mass of the car body and of the entire HSV can be expressed as:

$$\begin{aligned} W_{body,HSV} &= W_{body,CC}(P_{\max}, V) + \\ &- P_{\max}(m_g + m_{ICE}) - \Delta W \end{aligned} \tag{6}$$

$$\begin{aligned} W_{HSV} &= W_{body,HSV}(P_{\max}, V, \Delta W) + \\ &+ P_{EG}\left(\frac{m_{ICE}}{\eta_{EG}} + m_{EG}\right) + P_{\max} m_{EM} \\ &+ A_{PV} m_{PV} + m_B \cdot N_B \end{aligned} \tag{7}$$

The battery mass m_B is proportional to the number of modules needed to balance the maximum power of the reference vehicle (i.e. CC), estimated as follows:

$$N_B = \frac{P_{\max} - P_{EG}}{P_{B,u}} \tag{8}$$

where $P_{B,u}$ is the nominal power of a single battery module.

IV. COST ESTIMATION

In order to assess the benefits provided by HSV with respect to conventional vehicles, both the additional costs, due to hybridization and solar panels, and achievable fuel savings are to be estimated. The additional cost C_{HSV} can be expressed starting from the estimated unit cost of each component:

$$C_{HSV} = P_{EG}\left(\frac{c_{ICE}}{\eta_{EG}} + c_{EG}\right) + A_{PV}c_{PV} + P_{\max}c_{EM} + C_B N_B + \Delta W c_{al} + - \Delta C_{ICE} \quad (9)$$

The last two terms account for: i) reduction in chassis weight if aluminum is used [14] and ii) cost reduction for Internal Combustion Engine in HSV (where it is assumed $P_{ICE} = P_{EG}/\eta_{EG}$) with respect to conventional vehicle (where $P_{ICE}=P_{max}$).
The daily saving with respect to conventional vehicle can be computed starting from fuel saving and fuel unit cost:

$$S = \left(m_{f,CV} - m_{f,HSV}\right)\cdot c_f \quad (10)$$

The pay-back, in terms of years necessary to restore the additional costs with respect to the conventional vehicle, can be therefore estimated as:

$$PB = \frac{C_{HSV}}{n_D S} = \frac{C_{HSV}}{300S} \quad (11)$$

For further details about the meaning and the values of some of the parameters introduced in eqs. 2 through 11, the reader is addressed to a previous work [12].

V. VEHICLE DYNAMIC MODEL

In a previous paper [12], an extended optimization analysis was conducted to investigate the effects of latitude, costs, prices and layout on optimal vehicle structures, in terms of panel area, vehicle dimension and weight. The results presented have been obtained by computing the fuel saving of the HSV with respect to the conventional vehicle with a simplified approach, assuming average values for fuel consumption in the two cases [12], and average yearly solar data. This approach, although sufficient to assess the general feasibility of HSV and to understand the role of the main variables on costs and energy saving, does not allow accurate evaluation of the effects of vehicle weight and dimensions on inertial and aerodynamic forces during the driving cycle. Moreover, a more precise analysis is required to analyze the effects of control strategies on energy flows, also considering seasonal effects on solar energy. In order to overcome these limitations, a longitudinal vehicle model has been developed to simulate the dynamic behavior of both HSV and conventional vehicle over a driving cycle. Battery, electric motor and generator have been simulated by the ADVISOR model [15].

VI. ENGINE CONTROL FOR HSV

In most electric hybrid vehicles, a charge sustaining strategy is adopted: at the end of a driving path, the battery state of charge should remain unchanged. With a solar hybrid vehicle, a different strategy should be adopted, since battery can be charged during parking hours as well. In this case, a different goal can be pursued, namely restoring the initial state of charge within the end of the day rather than after a single driving path. For this end, the internal combustion engine should be operated whenever possible at maximum efficiency, corresponding to power P_{opt}. If the energy required to restore battery charge is lower than the amount corresponding to a continuous use at P_{opt} throughout the driving time h_d (case B), an intermittent operation can be adopted (cases A1-A2). In case that more energy is required, the internal combustion engine is operated at constant power between P_{opt} and P_{max} (case C). The different operating modes can be described by the variable ϕ, ranging from 0 to $\phi = P_{max} / P_{opt}$, as described in the table below.

TAB. II – Engine control strategies for HSV.

A1	$\phi < 1$	$P_{ICE} = 0$	$0 < t < \phi h_d$
A2	$\phi < 1$	$P_{ICE} = P_{opt}$	$\phi h_d < t < h_d$
B	$\phi = 1$	$P_{ICE} = P_{opt}$	$0 < t < h_d$
C	$1 < \phi < \phi_{\max}$	$P_{ICE} = \phi P_{opt}$	$0 < t < h_d$

The optimal ϕ value is found by imposing that the energy provided by ICE and PV panels during the driving hours guarantees a charge sustaining strategy over the whole day. This condition is expressed as:

$$\Delta SOC_{day}(\phi) = \int_0^{24h} dSOC(\phi)dt = = \Delta SOC_D(\phi) + \Delta SOC_p = 0 \quad (12)$$

Assuming that the driving schedule, long h_d hours, is composed of a sequence of ECE-EUDC cycles, eq. (12) can be satisfied by iteratively solving, over one cycle, the following nonlinear equation:

$$\Delta SOC_{ECE}(\phi) = \frac{-\left|\Delta SOC_p\right|}{N_{cycles}} \quad (13)$$

where N_{cycles} is evaluated as function of each module duration T_{cycle}:

$$N_{cycles} = \frac{h_d}{T_{cycle}} \quad (14)$$

FIGs 2 through 4 show the model outputs for a selected HSV configuration, simulated over an ECE-EUDC

driving cycle and controlled according to the strategies defined in TAB. II. FIG. 2 shows that the peaks in power demand are mainly met by the batteries.

FIG. 2 – Power contributions for the ECE-EUDC cycle ($A_{PV,H}$ = 4 m^2, P_{EG} = 13 kW, l = 3.5 m, w = 1.6 m, h =1.4 m).

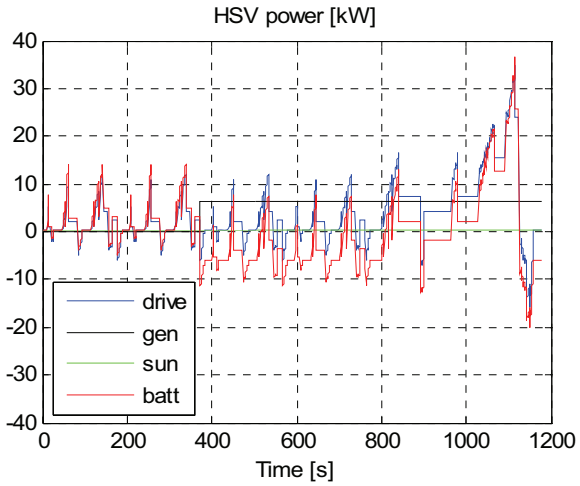

FIG. 3 – Comparison between CC and HSV rpm over the ECE-EUDC cycle ($A_{PV,H}$ = 4 m^2, P_{EG} = 13 kW, l = 3.5 m, w = 1.6 m, h =1.4 m).

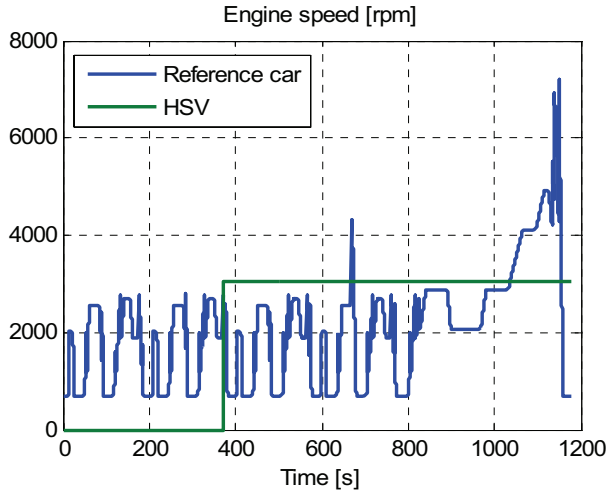

Since, for the selected case, the optimal ϕ is lower than one, the thermal engine can be operated at its highest efficiency in an intermittent way, as shown in FIG. 3 (green line). In the first part (i.e. in the time window 400-800 s), due the low-power demand, the ICE is mainly used to recharge batteries. Afterwards, it concurs with batteries to power the vehicle. In case of conventional vehicle (blue line), instead, the ICE works in most cases at partial loads, with higher values of specific fuel consumption. The resulting variation of battery state of charge (SOC) is shown in FIG. 4. Due to the constrained introduced by eq. (13), the final SOC differs from the initial value by a fraction of the amount of energy stored during the parking hours.

It is worth mentioning here that other strategies are possible, in case the ICE could run during parking mode too: in that case, the engine can be used to restore battery charge by working always at its maximum efficiency.

FIG. 4 – Battery state of charge ($A_{PV,H}$ = 4 m^2, P_{EG} = 13 kW, l = 3.5 m, w = 1.6 m, h =1.4 m).

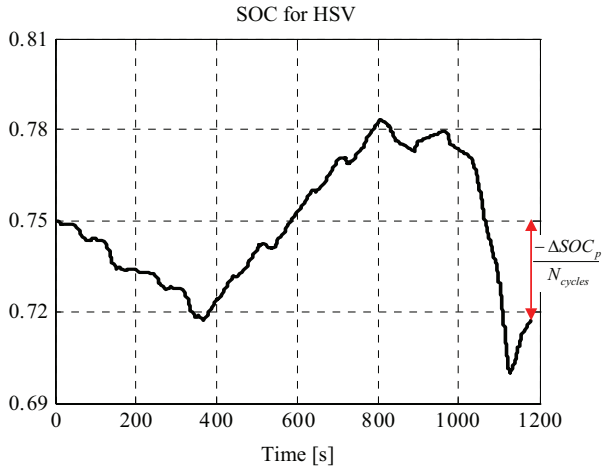

VII. PARAMETRIC ANALYSIS

In order to evaluate the energetic benefits of HSV configuration with respect to conventional vehicle, a parametric analysis has been carried out, ranging the electric generator (EG) power from 6 to 28 KW and the PV area from 0, corresponding to pure hybrid electric vehicle, to 4 square meters. The analysis has been performed by imposing a constant overall max power of 50 kW, therefore a decrease of EG power is compensated by an increase of battery modules. In this analysis, vehicle dimensions have been kept constantly equal to the reference vehicle ones (l = 3.5 m; w = 1.6 m; h = 1.4 m).

The analysis has been aimed at comparing the fuel consumption of conventional and Hybrid Solar vehicle, along a time horizon corresponding to the driving hours h_d. FIG. 5 shows the expected trend of vehicle mass vs. EG power: as the EG power is increased, the number of battery modules, needed to maintain the imposed maximum power, is reduced. This behavior results in a lighter vehicle since specific EG power (kW/kg) is greater than specific battery power. Furthermore the figure shows that the introduction of panels results in an increase of mass, almost linearly with PV area.

The behavior of the control variable ϕ with the EG power is shown in FIG. 6: according to the control strategy adopted, as the power is increased the EG provides the requested energy in a shorter time, thus reducing the operation time. Particularly, when the EG power is lower than 10 kW, the operation at the optimal power (P_{opt}) does not guarantee the requested energy. Thus, the EG is forced to work at a greater power with reduced efficiency (ϕ > 1). This behavior results in the fuel savings trends shown in FIG. 7, that evidence poor benefits in case of EG power lower than 10 kW. Furthermore, in case of conventional hybrid vehicle (PV area = 0), the fuel saving exhibits a negative value as the EG operation approaches the max power with very low efficiency (ϕ = 1.8). This negative trend is improved with the introduction of the panels that compensate for the EG low efficiency operation by recharging the batteries during parking hours.

FIG. 5 – Vehicle weight vs. electric generator power for different panels area.

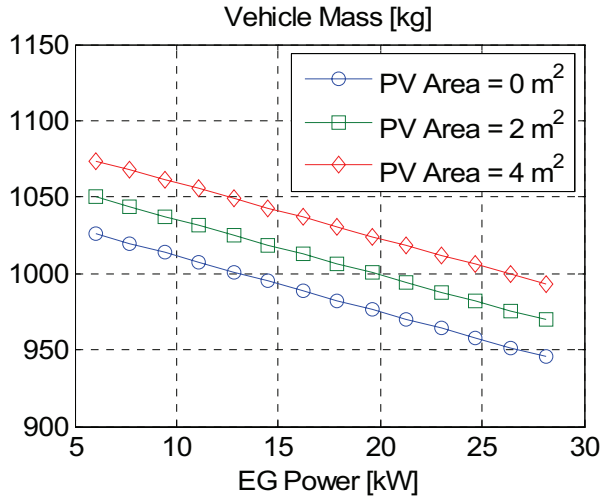

FIG. 6 – Control variable ϕ vs. electric generator power for different panels area.

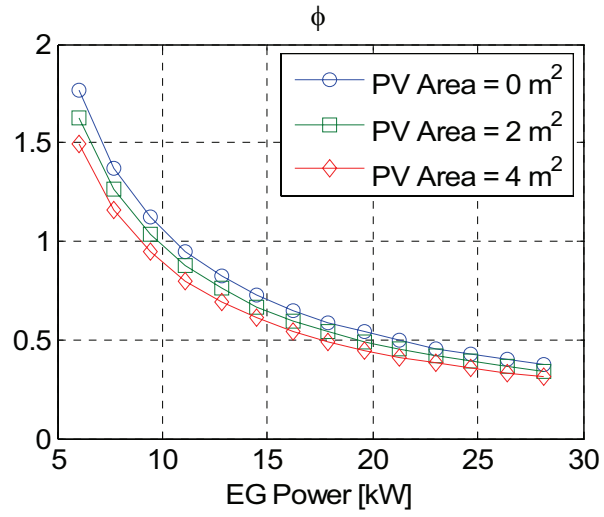

FIG. 7 – Fuel savings vs. electric generator power for different panels area.

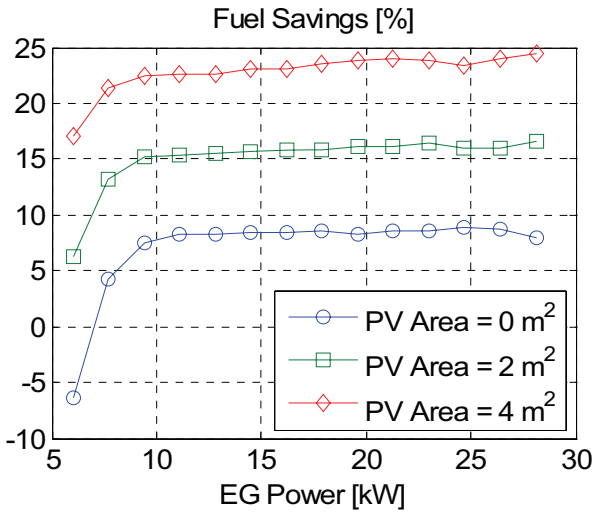

As the power is increased over 10 kW, the EG operates at max efficiency ($\phi < 1$) and the fuel savings exhibits an almost asymptotic trend. This behavior can be explained considering that, due to the negligible vehicle mass variation, the requested energy is almost constant and is provided with the same specific consumption in all cases where the control variable ϕ is lower than one. The figure also evidences that significant improvements of fuel economy can be achieved by introducing the panels, with max values approaching 25 % of savings with respect to conventional vehicle, in case of 4 m^2.

It can also be observed that the benefits achieved by the series hybrid vehicle without solar panels, with respect to the conventional vehicle, are relatively limited in this case, if compared with some results achieved by parallel HEV adopting advanced control strategies [8]. This result is due to the limited power adopted for the ICE in the conventional vehicle (50 KW), to the cascade energy losses associated to hybrid series structure and to the influence of driving cycle. Concerning the first effect, it is worth mentioning that the gain in fuel economy achievable by hybridizing a medium-high-power car (e.g. P_{max} = 70 kW) can reach up to 20%, which is more than double the increase obtained for the 50 kW vehicle analyzed in the current work (see FIG. 7). The influence of the driving cycle is also significant; in case of pure urban cycle, the gain in fuel economy for the same vehicle (50 KW) reaches 25 %. This is due to both the operation of the conventional vehicle ICE at poor efficiency and the higher benefits of regenerative braking in urban driving.

VIII. Optimization Approach

The models presented in the previous chapters allow to achieve the optimal design of the HSV via mathematical programming, considering both technical and economic aspects. The payback is assumed as objective function, while design variables X are represented by electric generator power P_{EG}, horizontal panel area $A_{PV,H}$ and car dimensions (l,w,h).

$$\min_X PB(X) \tag{15}$$

$$G_i(X) \le 0 \qquad i = 1, N_G \tag{16}$$

The inequality constraints G_i express the following conditions:

i) Car dimensions, length to width and height to width ratios within assigned limits, as addressed by the available database on commercial vehicles.

ii) PV panels area compatible with car dimensions, according to the given geometrical model.

A. Optimization analysis

The optimization analysis has been carried out by minimizing the PB evaluated by eq. (11). The reference vehicle considered to evaluate the daily saving (i.e. eq. 10) has the following specifications: $P_{ICE} = P_{max}$ = 50kW; $W_{body,CC}$ = 900 kg; l = 3.5 m; w = 1.6 m; h = 1.4 m. TAB. III summarizes the results applying the optimization criteria defined through eqs. (15) and (16).

Case 1, representing a series HEV without solar panels, is considered as reference, with a payback of 6.74 years with respect to the conventional vehicle. The addition of solar panels (e.g. case 2, $A_{PV,H}$ = 2 m^2) allows getting a 13% contribution from solar energy, but results in a

higher payback (from 6.74 to 10.63 years), due to the actual costs of fuel and panels.

TAB. IIII – Optimization results for different fuel cost and PV technology scenarios.

#	c_f [€/kg]	c_{PV} [€/m^2]	η_P [/]	$A_{PV,H}$ [m^2]	P_{EG} [kW]	PB [yrs]	λ [%]
1	1.77	800	0.13	0	9.14	6.74	0
2	1.77	800	0.13	2	9.14	10.63	13.12
3	1.77	200	0.13	3.63	10	6.14	20.27
4	3.54	200	0.16	5.85	7.64	2.25	31.09

The HSV can represent the optimal solution considering the occurrence of one (case 3) or all (case 4) of the following circumstances: a) PV cost reduction (by a factor 4); b) fuel cost doubling (by a factor 2); c) panel efficiency increase from 0.13 to 0.16. The variations in prices and costs are significant but not unrealistic, considering actual trends of reduction of solar component costs and increase in oil prices.
The model allows to estimate the optimal vehicle dimensions as well: while for case 1 a reduction in dimensions with respect to base case has been proposed, to reduce vehicle weight and aerodynamic losses, in case 4 larger values are adopted (l=3.85, w=1.73; h=1.39), compatible with the selected solar panel area (5.85 m^2).

CONCLUSIONS

A comprehensive model for the study and the optimal design of a solar hybrid vehicle with series architecture has been presented. The model describes energy flows between horizontal and/or vertical solar panels, internal combustion engine, electric generator, electric motor and batteries, considering vehicle longitudinal dynamics and the effect of control strategies. Vehicle weight is predicted, starting from a database of commercial vehicles, considering the effects of power-train sizing, vehicle dimensions and possible use of aluminum. The effects of vehicle dimensions on aerodynamic losses and maximum panel area also can be accounted for. The model predicts the additional costs with respect to conventional vehicles, and the pay-back.
It has been shown that significant savings in fuel consumption and emissions can be obtained with an intermittent use of the vehicle at limited average power, compatible with typical use in urban conditions during working days. This result has been obtained with commercial PV panels and with realistic data and assumptions on the achievable net solar energy for propulsion. The future adoption of last generation photovoltaic panels, with nominal efficiencies approaching 35%, may result in an almost complete solar autonomy of this kind of vehicle for such uses. By adopting up to date technology for electric motor and generator, batteries and chassis, power to weight ratio comparable with the ones of commercial cars can be achieved, thus assuring acceptable vehicle performance.
Future developments may concern a systematic study of optimal configuration for various driving cycles and latitudes, also considering seasonal variations of the solar energy, more accurate study of control strategies, including possible application of on-board optimization coupled with provisional methods for car load and solar energy based on Recurrent Neural Network. More detailed models for component weights and costs, including non-linear effects, also can be necessary, as well as further studies on the interactions between vehicle and propulsion system.
The results obtained by optimization analysis over a ECE/EUDC cycle have shown that the hybrid solar vehicles, although still far from economic feasibility, could reach acceptable payback values if large but not unrealistic variations in costs, prices and panel efficiency will occur: considering recent trends in renewable energy field and actual geo-political scenarios, it is reasonable to expect further reductions in costs for PV panels, batteries and advanced electric motors and generators, while relevant increases in fuel cost could not be excluded. Moreover, the recent and somewhat surprising commercial success of some electrical hybrid cars indicates that there are grounds for hope that a significant number of users is already willing to spend some more money to contribute to save the planet from pollution, climate changes and resource depletion.
In order to validate the model, a prototype of Hybrid Solar Vehicle with series structure is being developed at DIMEC, within a project funded by EU [16].

REFERENCES

[1] Hammad M., Khatib T. (1996), Energy Parameters of a Solar Car for Jordan, *Energy Conversion Management*, **V.37**, No.12.
[2] Wellington R.P. (1996), Model Solar Vehicles Provide Motivation for School Students, *Solar Energy* **Vol.58**, N.1-3.
[3] Saitoh, T.; Hisada, T.; Gomi, C.; Maeda, C. (1992), Improvement of urban air pollution via solar-assisted super energy efficient vehicle. *92 ASME JSES KSES Int Sol Energy Conf.* Publ by ASME, New York, NY, USA.p 571-577.
[4] Sasaki K., Yokota M., Nagayoshi H., Kamisako K. (1997), Evaluation of an Electric Motor and Gasoline Engine Hybrid Car Using Solar Cells, *Solar Energy Material and Solar Cells* (**47**), 1997.
[5] Seal M.R. (1995), Viking 23 - zero emissions in the city, range and performance on the freeway. *Northcon - Conference Record 1995. IEEE, RC-108*.p 264-268.
[6] Seal M.R., Campbell G. (1995), Ground-up hybrid vehicle program at the vehicle research institute. Electric and Hybrid Vehicles - Implementation of Technology *SAE Special Publications n 1105 1995*.SAE, Warrendale, PA, USA.p 59-65.
[7] S.Letendre, R.Perez, Christy Herig, Vehicle Integrated PV: a Clean and Secure Fuel for Hybrid Electric Vehicles, *Proc. of Annual Meeting of the American Solar Energy Society, June 21-26, 2003, Austin, TX.*
[8] Arsie I., Graziosi M., Pianese C., Rizzo G., Sorrentino M. (2004), Optimization of Supervisory Control Strategy for Parallel Hybrid Vehicle with Provisional Load Estimate, *Proc. of AVEC04*, Arhnem (NL), Aug.23-27, 2004.
[9] Statistics for Road Transport, UK Government, http://www.statistics.gov.uk/CCI/nscl.asp?ID=8100
[10] http://ww.itee.uq.edu.au/~serl/UltraCommuter.html
[11] Arsie I., Di Domenico A., Marotta M., Pianese C., Rizzo G., Sorrentino M. (2005); *A Parametric Study of the Design Variables for a Hybrid Electric Car with Solar Cells,* Proc. of METIME Conference, June 2-3, 2005, University of Galati, RO.
[12] Arsie I., Marotta M., Pianese C., Rizzo G., Sorrentino M. (2005); *Optimal Design of a Hybrid Electric Car with Solar Cells,* Proc. of 1st AUTOCOM Workshop on Preventive and Active Safety Systems for Road Vehicles, Istanbul, Sept.19-21, 2005.
[13] Marion B. and Anderberg M., "PVWATTS – An online performance calculator for Grid-Connected PV Systems", *Proc.of the ASES Solar 2000 Conf.*, June 16-21, 2000, Madison, WI.
[14] http://www.autosteel.org/articles/2001_audi_a2.htm
[15] Burch, S., Cuddy, M., Johnson, V., Markel, T., Rausen, D., Sprik, S., and Wipke, K., 1999, "ADVISOR: Advanced Vehicle Simulator", available at:http://www.ctts.nrel.gov.
[16] Leonardo Program I05/B/P/PP-154181 "Energy Conversion Systems and Their Environmental Impact", http://www.dimec.unisa.it/leonardo